npj | clean water

www.nature.com/npjcleanwater

ARTICLE OPEN

Check for updates

Development of softening and ballasted flocculation as a pretreatment process for seawater desalination through a reverse osmosis membrane

Tomohiro Yadai[1] and Yoshihiro Suzuki[1]✉

Efficient desalination through a reverse osmosis (RO) membrane requires the prior removal of blockade-causing substances from raw seawater. To achieve ultrahigh-speed processing of a pretreatment process for seawater RO desalination, we combine traditional softening with ballasted flocculation (SBF) for Ca^{2+} and Mg^{2+} removal. An alkaline mixture of $Ca(OH)_2$ and Na_2CO_3 was the most suitable softening agent for Ca^{2+} and Mg^{2+} removal with a reduced amount of generated sludge. This softening treatment simultaneously removed the suspended solids and bacteria from actual seawater. The settling velocity of the suspended solids generated via seawater softening was extremely low. Under the optimum conditions for desalinating actual seawater using an anionic polymer flocculant and microsand, the settling velocity exceeded 3.5 cm/s, 833 times higher than that of softening without ballasted flocculation. The amount of sludge after standing for 3 min was 76.5% lower in SBF than in conventional softening. The silt density index of the treated seawater met the water-supply standard of RO membranes (i.e., <3.0). Furthermore, the SBF-generated sludge exhibited considerably improved dewatering property than the sludge obtained via conventional softening. SBF can efficiently and quickly remove the causative substances of RO membrane fouling from seawater, thereby improving the treatability of generated sludge. SBF provides a new pretreatment process for seawater desalination using RO membranes.

npj Clean Water (2023)6:7 ; https://doi.org/10.1038/s41545-023-00226-0

INTRODUCTION

With the rapid increase in the global population, freshwater resources are increasingly demanded for households, agricultural activities, and industries[1]. One-fifth of the global population is currently facing water shortages[2]. Therefore, technologies that produce freshwater from the vast amount of seawater are urgently required[3]. Reverse osmosis (RO) is an energy-saving, highly economical, and energy-efficient desalination technology for seawater[4], with a high freshwater-recovery rate[5]. Accordingly, the RO membrane process is commonly used in desalination facilities[6] and is recognized as an important technology for seawater desalination. However, seawater desalination using RO membranes is prone to membrane fouling[7,8]. The main mechanism of membrane fouling is blockage due to scale formation by Ca^{2+} and Mg^{2+} ions, which are highly concentrated in seawater, and by inorganic substances such as silica and carbonates. Another problem is blockage by the organic matter[9] contained in seawater and bacterial biofilms[10,11].

RO membrane fouling increases the operating costs[12] and duration of washing the membrane; decreases the membrane lifespan, flow rate[13], and water permeation flux[14]; and deteriorates the permeated water quality. These problems seriously reduce the volume of freshwater production[15]. Therefore, prior to the RO membrane process, the causative substances of fouling must be removed from clogging substances using a pretreatment process[16]. In modern conventional pretreatments, seawater is treated with acids and/or scale inhibitors that lowers its pH and prevents scale formation by inorganic substances[17–19]. Suspended solids and colloidal particles can be removed using a combined coagulation and ultrafiltration membrane process[20], coagulation and sand filtration[21], or a dual-media filter comprising sand and cartridge filters[22]. However, these pretreatment processes cannot remove high concentrations of Ca^{2+} and Mg^{2+} ions (the causative agents of scale generation) from seawater[23]. Although chlorination can control biofouling[24], residual chlorine damages the RO membrane[25]. Therefore, to improve the efficiency of seawater desalination, a new pretreatment process that can easily and rapidly remove fouling substances from seawater without damaging the RO membrane is required.

Ayoub et al.[26] introduced softening as a pretreatment process in RO membrane-based desalination. Softening has been long used to remove Ca^{2+} and Mg^{2+} from industrial wastewater and hard water[27–32]. The softening method employs alkaline agents such as sodium hydroxide (NaOH) or calcium hydroxide ($Ca(OH)_2$), which removes Ca^{2+} and Mg^{2+} ions in seawater as insoluble salts. Moreover, agglutination of the produced insoluble hydroxides or carbonates reduces the turbidity and bacterial amounts. Therefore, softening is an attractive pretreatment option in seawater desalination via the RO membrane process. However, seawater softening methods have not progressed because the sedimentation process is slow and generates a large amount of sludge[33]. Owing to the robustness of seawater softening to salinity fluctuations, the neutralization of strong alkali-treated seawater, and the characteristics of the generated sludge are unknown. Resolving these disadvantages would promote seawater softening as a new pretreatment process in RO membrane-based desalination.

Ballasted flocculation (trade-named ACTIFLO) was introduced as an innovative solid–liquid separation process in the 1990s[34].

[1]Department of Civil and Environmental Engineering, Faculty of Engineering, University of Miyazaki, Gakuen Kibanadai-Nishi 1-1, Miyazaki 889-2192, Japan.
✉email: ysuzuki@cc.miyazaki-u.ac.jp

ACTIFLO uses microsand and a polymer flocculent to form large flocs with a high specific density, thereby accelerating the sedimentation. Ballasted flocculation has extracted purified water from polluted wastewater in various solid–liquid separation processes[35–39]. Veolia Water Technologies developed a method based on combined softening and ballasted flocculation that reduces the hardness of drinking and industrial water[40]. Although technologies exist for the softening (Ca^{2+} and Mg^{2+} removal) of hard freshwater, no technology can currently remove Ca^{2+}, Mg^{2+}, and other inhibitory substances from seawater prior to RO membrane-based seawater desalination. Moreover, the optimum conditions for seawater softening and the information related to disposal of generated sludge also remain unknown. We propose that the fine precipitates of insoluble hydroxides and carbonates generated via seawater softening can be settled at high speed via ballasted flocculation. Additionally, the large flocs formed by the polymer flocculant should reduce the sludge volume and improve dehydration[41].

To test these proposals, we developed an ultrahigh-speed pretreatment technology for RO membrane-based desalination based on softening with ballasted flocculation (SBF). The study proceeds through the following steps: (1) selection of an alkaline agent and optimization of the seawater softening conditions, (2) selection of the polymer coagulant and optimization of the SBF conditions, (3) characterization of water quality after the SBF treatment, (4) evaluation of sludge generation and dehydration using SBF, (5) neutralization of the strongly alkaline treated water using carbon dioxide gas, and (6) estimation of the silt density index (SDI) of the treated water. Collectively, these steps describe a new pretreatment process for RO membrane–based desalination.

RESULTS AND DISCUSSION

Removal of Mg^{2+} and Ca^{2+} using softening agents

Figure 1 shows the pH dependences of the Mg^{2+} and Ca^{2+} concentrations after adding different alkaline agents to the water samples. Mg^{2+} was effectively removed by all agents and the Mg^{2+} concentration dropped below the lower detection limit (Mg^{2+} < 0.057 mg/L) above pH 11. During the softening process, hydroxide ions (OH^-) were supplied to the seawater and Mg^{2+} was removed from the liquid phase as insoluble magnesium hydroxide ($Mg(OH)_2$). However, Ca^{2+} was not removed after adding NaOH and $Ca(OH)_2$. The Ca^{2+} concentration increased with increasing injection rate of $Ca(OH)_2$, exceeding the upper limit of 700 mg/L on the vertical axis in Fig. 1. Conversely, the $Ca(OH)_2 + Na_2CO_3$ and $NaOH + Na_2CO_3$ agents effectively removed Ca^{2+}. Above pH 11, the Ca^{2+} concentration of the samples softened with the mixed agents was below the lower detection limit (Ca^{2+} < 0.065 mg/L). Under alkaline conditions, Ca^{2+} reacted with CO_3^{2-} to form insoluble $CaCO_3$. The optimum addition volumes of the $Ca(OH)_2 + Na_2CO_3$ and $NaOH + Na_2CO_3$ agents for Ca^{2+} and Mg^{2+} removal were 40 and 72 mL per 1000 mL of seawater, respectively.

Generated amounts of suspended solids (SS) and sludge volume

Figure 2 shows the SS amounts and sludge volumes after 60 min of settling (SV_{60min}) generated after adding each alkaline agent and adjusting the pH to 11. After adding Na_2CO_3, the SS content doubled from that of the sample without Na_2CO_3. Statistically equivalent SS contents were obtained after adding $Ca(OH)_2 + Na_2CO_3$ and $NaOH + Na_2CO_3$ ($p > 0.05$). The Na_2CO_3 additive increased the SS content in seawater by forming $CaCO_3$. Comparing the sludge amounts generated by the $Ca(OH)_2 + Na_2CO_3$ and $NaOH + Na_2CO_3$ agents, the SV_{60min} in the $Ca(OH)_2 + Na_2CO_3$ system was 25.2%, one-third of that in the $NaOH + Na_2CO_3$ system.

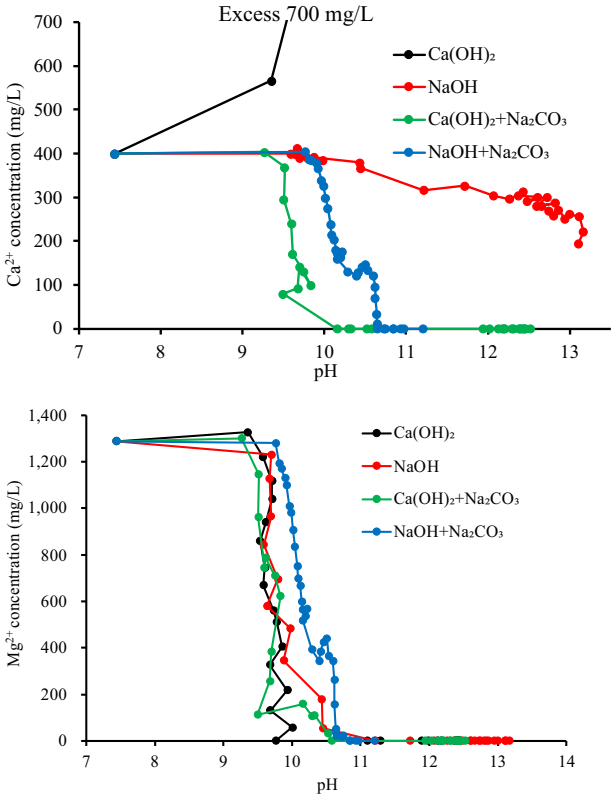

Fig. 1 Concentrations of Ca^{2+} (top) and Mg^{2+} (bottom) versus pH during softening with ballasted flocculation (SBF) using different alkaline agents. The alkaline agents were $Ca(OH)_2$ (dosage = 1.7 mol/L; dosage volume 1–32 mL), NaOH (5.0 mol/L; 1–22 mL), $Ca(OH)_2 + Na_2CO_3$ ($Ca(OH)_2$ = 1.7 mol/L; Na_2CO_3 = 2.0 mol/L, 1–40 mL), and $NaOH + Na_2CO_3$ (NaOH = 1.35 mol/L; Na_2CO_3 = 0.675 mol/L, 1–72 mL).

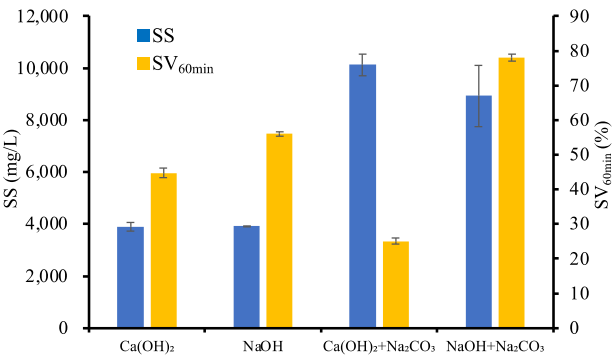

Fig. 2 Suspended solids (SS) and sludge volumes after 60 min of settling time (SV_{60min}) for each alkaline agent after pH adjustment to 11.0. (n = 3, means ± standard deviations).

The system using NaOH produced sludge with more pore water and a lower specific gravity than the system using $Ca(OH)_2$. Ayoub and Merhebi[33] reported high compressive properties in $Ca(OH)_2$-treated sludge. Relative to the other alkaline agents in this study, $Ca(OH)_2 + Na_2CO_3$ reduced the sludge volume SV_{60min} by more than half. Furthermore, using NaOH yielded residual Na^+ in the treated water. To achieve the desired low amount of sludge generation with no accumulation of Na^+, we selected $Ca(OH)_2 + Na_2CO_3$ as the most suitable alkaline agent for softening treatment of seawater.

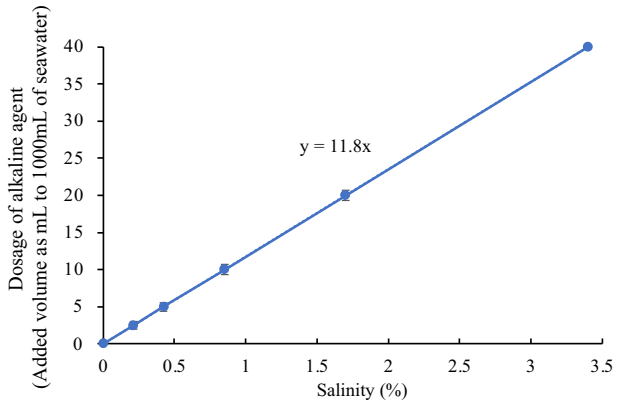

Fig. 3 Relationship between optimum dosage of the best alkaline agent ($Ca(OH)_2 + Na_2CO_3$) and seawater salinity ($n = 3$, means ± standard deviations). Salinity was adjusted (0–3.5%) by diluting artificial seawater with distilled water.

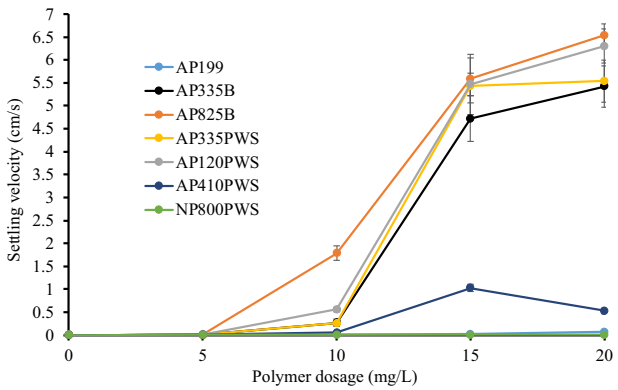

Fig. 4 Floc settling velocity versus flocculent dosage for different polymer flocculants in softening with ballasted flocculation (SBF) of artificial seawater ($n = 3$, means ± standard deviations). Six types of anionic polymers (AP199, AP335B, AP825B, AP335PWS, AP120PWS, and AP410PWS) and one nonionic polymer (NP800PWS) were tested.

Relation between salinity and dosage of alkaline agent

The alkaline-agent dosage in the softening treatment depends on the Mg^{2+} and Ca^{2+} concentrations in the seawater. Therefore, we investigated the optimum dosage of the alkaline agent at different salinities in artificial seawater. At the optimum dosage, the Mg^{2+} and Ca^{2+} concentrations were reduced to below the lower detection limit. As the optimum dosage of the alkaline agent was strongly linearly correlated with salinity (Fig. 3), the optimum dosage of the alkaline agent could be determined from the salinity of the seawater. Applying the correlation presented in Fig. 3 to actual seawater, in which the softening effect can be inhibited by turbidity and bacteria, the optimum dosage rate of the alkaline agent was determined to be 100%. The softening treatment was further examined at alkaline-agent dosage rates of 110%, 120%, 130%, 140%, and 150%. Supplementary Fig. 1 shows the Mg^{2+} and Ca^{2+} concentrations in three samples of actual seawater during softening at alkaline-agent dosage rates of 100–150%. At the 100% dosage rate, the Mg^{2+} and Ca^{2+} concentrations decreased considerably but the ions were not completely removed from the treated water. Conversely, at dosage rates above 120%, no Mg^{2+} or Ca^{2+} was detected in the treated water. Based on these results, the optimum dosage of the alkaline agent in artificial seawater was multiplied by 1.2 (120%) to obtain the optimum dosage in actual seawater.

Treated-water quality of the actual seawater samples after softening

Supplementary Table 1 shows the treated-water qualities after softening the seawater samples collected from different sampling points. Mg^{2+} and Ca^{2+} were almost completely removed from all actual seawater samples (removal rates ≈ 100%). The K^+ removal rate was very low (3.8–6.8%) and the Na^+ removal rate was zero (in fact, the alkaline agent increased the Na^+ concentration in the treated seawater by contributing Na^+ ions). Meanwhile, the SS aggregated with the generation of $Mg(OH)_2$ and $CaCO_3$, affording high turbidity removal efficiency. Furthermore, no *Escherichia coli* and total coliforms were detected in the treated seawater and the number of heterotrophic bacteria was reduced by 95.9–100%. Ayoub et al.[26] similarly reported the complete removal of total and fecal coliforms above pH 10.5. Therefore, the softening treatment can simultaneously remove Mg^{2+} and Ca^{2+}, SS, and bacteria from actual seawater. However, the settling velocity of the SS generated by the seawater softening treatment was extremely low. Additionally, the SV_{60min} exceeded 29% and the amount of generated sludge was large.

Optimization of SBF

Figure 4 plots the floc settling velocity versus dosage of each polymer flocculant in the SBF process using artificial seawater. Herein, the optimum dosage of the alkaline agent and 10 g/L of the microsand were added to artificial seawater. When added at 15 mg/L, the four polymer flocculants AP335B, AP825B, AP335PWS, and AP120PWS, which have high and medium degrees of anionic strength (Supplementary Table 2), formed large flocs with considerably increased settling velocities (>4.5 cm/s). When added at 20 mg/L, the AP825B and AP120PWS flocculants further increased the settling velocity to above 6 cm/s. For comparison, the settling velocity in the absence of a polymer flocculant was only 2.8×10^{-3} cm/s. Ballasted flocculation of the artificial seawater increased the settling velocity by a factor of 1.9×10^3–2.3×10^3. The floc settling velocity was maximized (at 6.5 cm/s) by adding 20 mg/L of AP825B polymer. AP825B has the lowest molecular weight among the four polymer flocculants with high and medium degrees of anionic strength. The low water content of the formed flocs indicates a high specific gravity of the flocs. Conversely, the anionic polymer flocculant AP119, which has extremely high anionic strength, and the nonionic NP800PWS exerted no ballasted flocculation effect. Anionic polymers with extremely high ionic strength and nonionic polymers cannot combine the microsand with the aggregates of magnesium hydroxide and calcium carbonate generated under the alkaline conditions of seawater.

Figure 5 compares the volumes of sludge generated in the systems with various polymer flocculants after 3 min of settling (SV_{3min}). In the absence of a polymer flocculant, the settling velocity of the flocs was extremely low and settling was barely observed after 3 min ($SV_{3min} = 99.0\%$). The polymer flocculants accelerated the floc sedimentation and markedly decreased the SV_{3min} as their dosage increased. When dosed at 20 mg/L, the four specified high- and medium-anion polymer flocculants, which accelerated the floc settling velocity, produced small amounts of sludge (<25%) than the other flocculants. Among the four polymer flocculants, AP335B and AP825B achieved the lowest SV_{3min}s, averaging 21.5% and 22.0%, respectively, with no significant difference between the two values ($p > 0.05$). Conversely, the nonionic polymer NP800PWS, which could not form flocs, generated a large amount of sludge. Based on the settling velocities and SV_{3min} values of the flocs, AP825B was determined as the most suitable polymer flocculant for the SBF treatment of seawater.

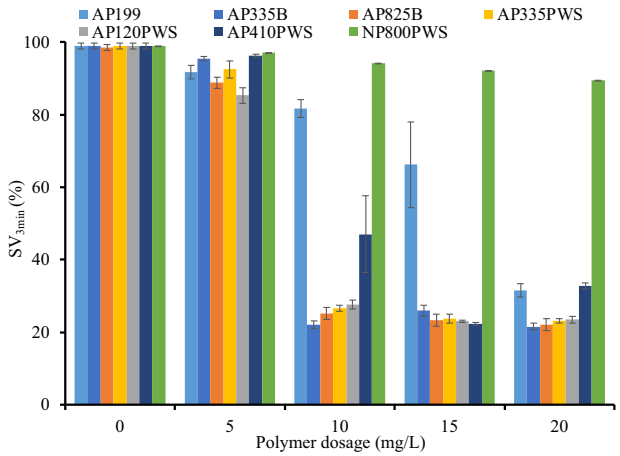

Fig. 5 Sludge volumes generated after 3 min of settling (SV_{3min}) in softening with ballasted flocculation (SBF) with different dosages of various polymer flocculants (color coded) ($n = 3$, means ± standard deviations). Six types of anionic polymers (AP199, AP335B, AP825B, AP335PWS, AP120PWS, and AP410PWS) and one nonionic polymer (NP800PWS) were tested.

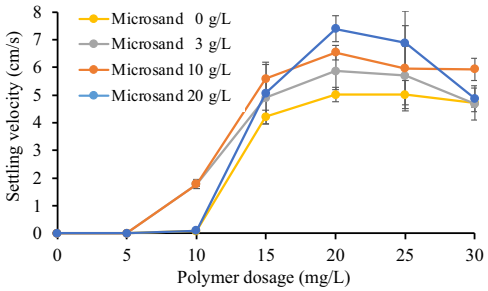

Fig. 6 Relationships between floc settling velocity and polymer flocculant dosage in softening with ballasted flocculation (SBF) with different micros and dosages ($n = 3$, means ± standard deviations). Anionic polymer (AP825B) was used in SBF.

Relation between floc settling velocity and sludge-generation volume at different microsand dosages

The settling velocity of the flocs was considered to depend on the microsand dosage. Therefore, the floc settling velocity was investigated in SBF using the AP825B flocculant with different dosages of microsand (0, 3, 10, or 20 g/L). Figure 6 relates the settling velocity of the flocs to the flocculant dosage at each microsand dosage. At all microsand dosages, polymer dosages >15 mg/L produced large flocs with considerably increased settling velocities. The settling velocity depended on the microsand dosage and was maximized at 7.4 cm/s in the SBF with 20 g/L of microsand. Excess anionic polymer (>25 mg/L) caused electrostatic repulsion among the negatively charged particles, thereby hindering the floc formation and ultimately reducing the settling velocity. Therefore, determining the appropriate amount of polymer flocculant at a given microsand dosage is an important step in SBF treatment.

Supplementary Fig. 2 compares the sludge volumes generated in the systems with different microsand dosages. The SV_{3min} decreased considerably at polymer flocculant dosages exceeding 10 mg/L. At polymer dosages of 15 and 20 mg/L, increasing the microsand dosage to 10 g/L decreased the amount of sludge to 20% because the increased specific density of the flocs caused compressive settling. However, in the system with 20 mg/L of polymer, the SV_{3min} values were not significantly different at microsand dosages of 10 and 20 g/L ($p > 0.05$). Based on the observed floc settling velocities and SV_{3min} values, the optimum polymer flocculant and sand dosages of the SBF were determined to be 20 and 10 g/L, respectively.

Neutralization of the alkaline agent–treated water

The treated water generated in SBF is highly alkaline and must be neutralized. Herein, the treated water was neutralized under optimum conditions. The pH changes during neutralization with sulfuric acid (H_2SO_4) and carbon dioxide (CO_2) are shown in Supplementary Fig. 3. After neutralization with H_2SO_4, the pH dropped sharply because H_2SO_4 was added in excess, resulting in acidification. Additionally, as H_2SO_4 is a deleterious substance, restrictions are imposed on its use. Conversely, during aeration neutralization with CO_2 gas, the pH decreased to 5.8 and remained at 5.8 with further aeration. This experiment required 2.0 g (gas volume = 1.0 L) of CO_2 to neutralize 1000 mL of softened seawater through simple aeration of the samples in a beaker. Treated water is easily neutralized by CO_2, a harmless gas. Based on these results, CO_2 gas was selected as the neutralizer of actual seawater after processing via SBF.

Application of SBF to actual seawater

After softening and ballasted flocculation under optimum conditions, the settling velocity of actual seawater exceeded 3.5 cm/s, 833 times higher than the settling velocity after softening without ballasted flocculation. The SV_{3min} values for all samples were <32.5%. The SBF treatability results of each water-quality parameter in the actual seawater samples are given in Table 1. The treatability results matched those of the softening treatment (Supplementary Table 1). Mg^{2+} and Ca^{2+} were almost completely removed from all actual seawater samples (removal rates of ~100%). The removal rate of SiO_2 was low at Miyazaki Port (averaging 23.6% over three samples). The dissolved SiO_2 detected by the employed silicate molybdic acid method exists in ionic, molecular, and colloidal chemical forms. The ionic fraction of SiO_2 can be removed during aggregation via electrostatic adsorption by $Mg(OH)_2$ used in the softening process. Conversely, the Na^+ concentration was higher in the treated water than in the raw seawater because it was contributed by the alkaline softening agent. Meanwhile, the turbidity was rapidly removed because the SS were aggregated with the insoluble $Mg(OH)_2$ and $CaCO_3$ products of softening. No *E. coli* and total coliforms were detected in the treated water, and the numbers of heterotrophic bacteria were reduced by 88.0–99.5%. Two mechanisms of bacterial removal from water are proposed here: (1) Inactivation and death of most bacterial species under strongly alkaline conditions (pH ≥11) and (2) sequestering of bacteria in the floc aggregates formed by $Mg(OH)_2$. Therefore, SBF can efficiently remove Mg^{2+} and Ca^{2+}, SS, and bacteria from seawater.

Evaluation of SDI of actual seawater

To assess whether seawater treatment via SBF and neutralization with CO_2 is applicable to the RO membrane process, we computed the SDIs of the raw and treated seawater samples collected from Miyazaki Port, Aoshima Port, and the mouth of Tsukunami River. The results are presented in Supplementary Table 3. The SDI values of all raw seawater samples exceeded 5.7 (the upper limit of the SDI measurement device). Therefore, actual seawater should not be directly passed through the RO membrane. Conversely, the SDI values of the treated seawater samples were below 2.9. The SDI of water applied to RO membranes should not exceed the standard value, which is generally set below 3.0[42,43]. The SDI values determined in the present study confirmed that after pretreatment using SBF, the seawater met the water-supply standard of RO membranes.

Table 1. The treatability of SBF for each water quality parameter for actual seawater.

(a) Miyazaki Port.

Parameter	Unit	Miyazaki Port	
		Raw water	Treated water
		Mean ± SD ($n = 3$)	Mean ± SD ($n = 3$)
pH	–	$8.2 \pm 3.9 \times 10^{-2}$	$11.7 \pm 4.1 \times 10^{-2}$
EC	mS/cm	$37.9 \pm 9.4 \times 10^{-2}$	39.2 ± 0.33
Turbidity	ppm	1.8 ± 0.70	2.1 ± 0.35
SiO_2	mg/L	1.3 ± 0.25	1.4 ± 0.85
Mg^{2+}	mg/L	1488 ± 51.1	BDL*
Ca^{2+}	mg/L	464 ± 21.1	BDL
Na^{+}	mg/L	9985 ± 383.5	$12{,}695 \pm 245.3$
K^{+}	mg/L	376 ± 13.1	375 ± 13.0
E. coli	CFU/100 mL	5.3 ± 2.9	0
Coliforms	CFU/100 mL	57.3 ± 40.9	0
Heterotrophic bacteria	CFU/100 mL	$5.8 \times 10^4 \pm 2.5 \times 10^4$	$7.0 \times 10^3 \pm 8.2 \times 10^2$

(b) Aoshima Port

Parameter	Unit	Aoshima Port	
		Raw water	Treated water
		Mean ± SD (n = 3)	Mean ± SD (n = 3)
pH	–	$8.3 \pm 3.0 \times 10^{-3}$	$12.5 \pm 3.0 \times 10^{-2}$
EC	mS/cm	$40.6 \pm 9.4 \times 10^{-2}$	41.6 ± 0.49
Turbidity	ppm	$2.6 \pm 2.3 \times 10^{-2}$	0.93 ± 0.14
SiO_2	mg/L	$1.1 \pm 9.4 \times 10^{-2}$	0.6 ± 0.24
Mg^{2+}	mg/L	1595 ± 6.0	BDL
Ca^{2+}	mg/L	474 ± 2.1	BDL
Na^{+}	mg/L	$11{,}105 \pm 138.2$	$13{,}539 \pm 163.4$
K^{+}	mg/L	386 ± 1.0	358 ± 3.7
E.coli	CFU/100 mL	0	0
Coliforms	CFU/100 mL	5.3 ± 2.1	0
Heterotrophic bacteria	CFU/100 mL	$3.2 \times 10^4 \pm 3.1 \times 10^4$	$6.7 \times 10^2 \pm 9.4 \times 10^2$

(c)Tukunami River

Parameter	Unit	Tsukunami River	
		Raw water	Treated water
		Mean ± SD (n = 3)	Mean ± SD (n = 3)
pH	–	$8.4 \pm 4.5 \times 10^{-3}$	$11.9 \pm 3.0 \times 10^{-2}$
EC	mS/cm	36.7 ± 0.62	$37.0 \pm 9.4 \times 10^{-2}$
Turbidity	ppm	6.4 ± 0.84	1.5 ± 0.85
SiO_2	mg/L	1.3 ± 0.36	0.97 ± 0.52
Mg^{2+}	mg/L	1497 ± 5.7	BDL
Ca^{2+}	mg/L	464 ± 10.7	BDL
Na^{+}	mg/L	$10{,}450 \pm 110.0$	$12{,}415 \pm 101.8$
K^{+}	mg/L	383 ± 8.1	354 ± 3.6
E.coli	CFU/100 mL	13.3 ± 1.7	0
Coliforms	CFU/100 mL	50.3 ± 9.0	0
Heterotrophic bacteria	CFU/100 mL	$8.7 \times 10^5 \pm 8.2 \times 10^5$	$4.0 \times 10^3 \pm 8.2 \times 10^2$

**BDL* Below detection limit.

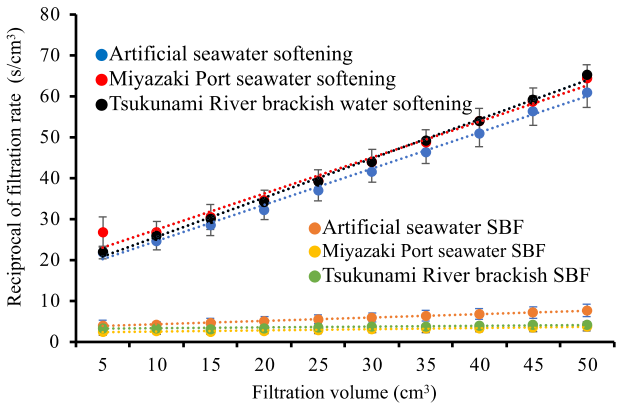

Fig. 7 Comparison of sludge dehydration in artificial and actual seawater samples after conventional softening and softening with ballasted flocculation (SBF), obtained in a Buchner funnel test ($n = 3$, means ± standard deviations).

Sludge dehydration

Finally, we compared the specific resistances of the sludges generated via conventional softening and SBF. Figure 7 shows the results of the Buchner funnel test on the artificial and actual seawater samples (Miyazaki Port and the mouth of Tsukunami River). When the reciprocal filtration rate was plotted against the amount of passing water, the sludges obtained after conventional softening of the artificial seawater and both types of actual seawaters yielded similar slopes (4.40–4.80), but the sludge obtained from SBF-based treatment of artificial seawater yielded a slope <1/10th that of the conventionally softened sludge. The decreased slope of the reciprocal filtration rate implies considerably improved water permeability of the sludge. The slope further decreased to 0.11–0.15 after SBF of the actual seawater samples. Supplementary Table 4 shows the Ruth constants[44] K and C obtained through the dehydration test of each sample. The K and C values indicate the filtration resistances of the sludge cake and filter medium, respectively. In the artificial seawater test, the K and C values were 9.9 and 2.1 times higher, respectively, for the SBF-generated sludge than for the conventionally softened sludge. For the sludges obtained from actual seawater, the K and C values were 34.5–45.5 and 3.9–8.9 times higher, respectively, after the SBF treatment than after conventional softening. The sludge generated via SBF exhibited extremely high permeability and considerably higher dehydration than the sludge formed using conventional softening.

Advantage of SBF

As a pretreatment process for RO membrane-based seawater desalination, we investigated an SBF treatment process that combines the existing softening process with ballasted flocculation–sedimentation for ultrahigh-speed precipitation. Based on the removal efficiencies of Ca^{2+} and Mg^{2+} and the amount of generated sludge, $Ca(OH)_2 + Na_2CO_3$ was determined as the best softening agent. The SBF process with the $Ca(OH)_2 + Na_2CO_3$ agent effectively removed Ca^{2+} and Mg^{2+} from actual seawater samples and reduced the turbidity and bacterial counts in the seawater. Furthermore, the seawater samples with different salinities could be treated by adjusting the dosage of the alkaline agent. The settling velocities of $Mg(OH)_2$ and $CaCO_3$ produced via conventional softening were extremely low and could not meet the requirements of pretreatment technologies for practical RO desalination.

Conversely, SBF achieved an 833-times higher settling velocity than conventional softening while achieving the same water quality. The optimum SBF conditions for treating seawater with a

Fig. 8 Locations of sampling points at Aoshima Port, Tsukunami River, Kizaki Beach, Shirahama Beach, Miyazaki Port, and Sun-Marina Port in Miyazaki City, Japan.

salinity of 3.5% were determined to be as follows: pH = 11, alkaline agent = $Ca(OH)_2 + Na_2CO_3$ dosed at 40 mL/L, anionic polymer flocculant = AP825B dosed at 20 mg/L, and microsand concentration = 10 g/L. The pH of the strongly alkaline treated seawater was reduced to pH 5.8 via aeration using CO_2 gas. The optimized SBF process reduced the SDI of seawater to below the standard value (3.0) and considerably improved the dewatering property of the generated sludge compared with that of the sludge obtained via conventional softening.

Dissolved substances such as Ca^{2+} and Mg^{2+} cannot be removed by the existing pretreatment methods for RO membranes (e.g., sand filtration and microfiltration membranes), which rely on physical filtration. Moreover, the sand and/or membrane must be cleaned to maintain the physical filtration performance. Conversely, SBF can efficiently and rapidly remove the causative substances of RO membrane fouling from seawater and can considerably improve the treatability of the generated sludge. We, therefore, propose SBF as a new pretreatment process for RO membrane-based seawater desalination. However, the optimum conditions and processing characteristics of SBF were obtained only in a laboratory jar test. As a next step, we must construct a practical system and examine its processing capacity during actual operation. Supplementary Fig. 4 shows the system flow of the RO membrane-based desalination applying ballasted flocculation. The system includes seawater intake; an SBF system consisting of an alkaline agent mixing tank, microsand mixing tank, flocculation tank, and inclined plate sedimentation tank; a neutralization device equipped with CO_2 aeration; and an OR membrane unit. We believe that the softening system, which has been already developed and used in various fields, can be combined with the proposed SBF to realize a practical SBF system.

METHODS

Seawater preparation

For basic studies and comparisons of SBF with conventional softening, we required raw water with a consistent water quality. Therefore, we prepared artificial seawater with the composition shown in Supplementary Table 5. The Ca^{2+} and Mg^{2+} concentrations were 400 and 1289 mg/L, respectively. Assuming that the method tested in artificial seawater will be used in practical applications, we collected actual seawater from six sites in Miyazaki City, Japan (Fig. 8): Aoshima Port (a small fishing port adjacent to a tourist beach), the mouth of the Tsukunami River (a brackish water area of a small river), Kizaki Beach (a sandy beach that serves as an international surfing venue), Shirahama Beach (a sandy beach), Miyazaki Port (the largest port in a berthing area for large vessels), and Sun-Marina Port (an artificial yacht harbor). At each site, the seawater samples were collected from the surface layer in a polyethylene container and transported to our laboratory in Miyazaki City for experimental study.

Agents

Softening can be performed using the lime aggregation method using calcium hydroxide ($Ca(OH)_2$) and sodium carbonate (Na_2CO_3)[45,46] and the soda aggregation method using sodium hydroxide (NaOH) and Na_2CO_3[26]. Therefore, four types of alkaline agents—$Ca(OH)_2$ alone, NaOH alone, mixed $Ca(OH)_2$ and Na_2CO_3 ($Ca(OH)_2 + Na_2CO_3$), and mixed NaOH and Na_2CO_3 ($NaOH + Na_2CO_3$)—were examined as softening agents in the present study. Furthermore, $Ca(OH)_2$ is the most widely used alkali agent in softening treatments. Additionally, NaOH is the most common alkaline water-treatment agent, and Na_2CO_3 insolubilizes Ca^{2+} ions through $CaCO_3$ formation. In the $Ca(OH)_2 + Na_2CO_3$ agent, the concentrations of $Ca(OH)_2$ and Na_2CO_3 were set to 1.7 and 2.0 mol/L, respectively, based on the conventional softening protocol concerning the Ca^{2+} and Mg^{2+} concentrations in artificial seawater[47]. In the $NaOH + Na_2CO_3$ agent, the NaOH and Na_2CO_3 concentrations were set to 1.35 and 0.675 mol/L, respectively, according to those reported by Ayoub et al.[26]. The single $Ca(OH)_2$ and NaOH agents were prepared at 1.7 and 5.0 mol/L, respectively.

Silica sand (quartz content >98%, specific gravity = 2.6, particle size = 53–212 μm, V7 type; Mikawakeiseki Co., Japan) was used as ballast in the microsand. As the polymer flocculants, we selected six types of anionic polymers (AP199, AP335B, AP825B, AP335PWS, AP120PWS, and AP410PWS; Mitsubishi Chemical Corporation, Japan) and one nonionic polymer (NP800PWS, Mitsubishi Chemical Corporation). The properties of the polymer flocculants are given in Supplementary Table 2. The concentration of each flocculant sample was adjusted to 0.1 w/v% by diluting its stock solution in distilled water.

Conventional softening and SBF

A 500- or 1000-mL beaker containing 500 or 1000 mL of water sample was set in a jar tester (JMD-8E, Miyamoto Riken Ind., Japan). A prescribed amount of each alkaline agent (single $Ca(OH)_2$ [dosage volume of stock solution = 1–32 mL], single NaOH [1–22 mL], $Ca(OH)_2 + Na_2CO_3$ [1–40 mL], and $NaOH + Na_2CO_3$ [1–72 mL]), was added to the sample under stirring. The sample was stirred rapidly (100 rpm) for 1 min and then slowly (30 rpm) for 20 min. The mixture was allowed to stand for 60 min to allow precipitate formation, and the supernatant water (named treated water) was gently collected using a syringe. To determine the appropriate dosages of alkaline agent for seawaters of different salinities, the artificial seawater was diluted to salinities of 0.34–3.4% using distilled water. The appropriate amount of added alkaline agent was determined at each salinity value. The jar test flows of softening and SBF are shown in Supplementary Fig. 5.

To ensure uniform stirring and mixing of the insoluble salt suspensions produced via softening and ballasted flocculation (using microsand and polymer flocculant), four baffle plates (width = 15 mm and height = 140 mm) were fixed inside the beaker. An alkaline agent was added to 1000 mL of the sample placed in a 1000-mL beaker set in a jar tester, and the resultant mixture was rapidly stirred (200 rpm) for 1 min. Subsequently, silica sand (0–20 g/L) was directly added, and after stirring at 200 rpm for 2 min, a prescribed dosage (0–20 mg/L) of polymer flocculant was injected into the samples. After injecting the polymer flocculant, the stirring speed was adjusted to 140 rpm and the mixture was further stirred for 3 min. After allowing the mixture to stand for 3 min, 100 mL of the supernatant water (treated water) was gently collected using a syringe (at 5 cm from the top of the supernatant).

Water-quality analysis

The pH values and electric conductivities of the samples were determined using a water-quality analyzer (LAQUA F-74, Horiba, Japan), and the turbidities were determined using a turbidity meter (PT-200, Nittoseiko Analytech, Japan). The Na^+, K^+, Mg^{2+}, and Ca^{2+} concentrations in the sample (diluted 100-fold with distilled water) were analyzed using an inductively coupled plasma emission spectroscopic analyzer (ICPS-8100, Shimadzu, Japan). The SiO_2 concentration was measured using a portable absorptiometer (DR-2800, Hach, U.S.) based on the silicate molybdic acid method according to the manufacturer's instructions. To obtain SS, 50 ml of the sample was passed through a glass fiber filter (GF/F; diameter = 47 mm; pore size = 0.7 µm, Whatman, Merck, Germany) and dried at 105 °C for 2 h. Bacterial counts were measured in the actual seawater. *E.coli* and total coliform colonies were counted after growth on CHROMagar ECC agar plates (CHROMagar, Paris, France). For this purpose, 100 mL of each water sample was filtered through a 0.45-µm pore size–membrane filter (47-mm diameter, sterile, mixed cellulose ester; Advantec, Tokyo, Japan) and incubated on ECC agar plates for 24 h at 37 °C. Blue colonies were designated as *E. coli* isolates and mauve colonies were designated as the isolates of other coliform species. Heterotrophic bacteria were counted on agar plates (1.5% agar, Difco Marine Broth 2216; Becton, Dickinson and Company, MD, USA). The seawater and treated-water samples were spread onto the plates and incubated for seven days at 22.5 °C ± 2.5 °C. After incubation, all colonies were counted as heterotrophic bacteria. The numbers of coliform bacteria, *E. coli*, enterococci, and heterotrophic bacteria in all samples were determined as the mean numbers of colony-forming units (CFUs) of three replicates. The bacterial count was expressed as CFU/100 mL water.

Determination of floc settling velocity and sludge volume

Immediately after slow stirring in the jar tester, the settling velocity of the flocs was measured as the settling depth (cm) at the interface between the floc suspension and supernatant water per unit time (cm/s). The settling velocity was reported as the average of three measurements in the jar test. If the floc settling velocity exceeded 2.0 cm/s (i.e., exceeded the measurable velocity of this approach), a 2000-mL glass cylinder (height = 50 cm) was filled with treated water and a portion of the sludge floc was separated and gently poured onto the water surface. The settling velocity was again measured as the settling depth per unit time. In the cylinder, the settling velocity was determined as the average of five measurements.

The sludge volume (SV) after a specified settling time (3 min for SV_{3min}; 60 min for SV_{60min}) was calculated as follows:

$$\mathrm{SV}(\%) = \text{sludge volume}\,(mL)/\text{sample water volume}\,(mL) \times 100.$$

Neutralization of treated seawater

Direct passage of the softened water (which is strongly alkaline) through the RO membrane increases the burden on the membrane and corrodes the water pipes[48]. To avoid these problems, the water must be neutralized prior to the RO membrane process. In this study, the neutralization agents were acid and carbon dioxide[49]. During neutralization with acid, the water pH was measured while dropwise adding a 1.0-mol/L H_2SO_4 solution to 1000 mL of treated water. During neutralization with CO_2, the pH was measured while passing CO_2 gas through 1000 mL of softened water (flow rate = 0.5 L/min).

SDI measurements

The SDI method is the usual method for evaluating the quality of water in the RO membrane process and stipulated in the American Society for Testing and Materials (ASTM)[50]. After neutralizing the treated water with CO_2, the SDI_{15} (where the subscript denotes 15 min of water passage) was determined using an SDI automatic measuring device (Simple SDI 2.0, Tosc Japan, Japan) under the ASTM regulation.

Buchner funnel test of specific resistance

The specific resistance of the sludge was evaluated via the Buchner funnel test using a Buchner funnel (diameter = 80 mm, height 160 mm) and a standard filter paper (diameter = 90 mm; No. 1, Advantec, Toyo Roshi Co., Japan). The Buchner funnel test was performed under gravity. A sludge sample generated from 1000 mL of seawater was added to the funnel and the filtration duration and amount of filtrate were determined. The dehydration tolerance of the sludge was evaluated in terms of the Ruth filtration constants K (cm^6/s) and C (cm^3)[44].

DATA AVAILABILITY

The data that support the findings of this study are available from the corresponding author upon reasonable request.

Received: 28 August 2022; Accepted: 23 January 2023;
Published online: 11 February 2023

REFERENCES

1. Park, K., Kim, J., Yang, D. R. & Hong, S. Towards a low-energy seawater reverse osmosis desalination plant: a review and theoretical analysis for future directions. *J. Membr. Sci.* **595**, https://doi.org/10.1016/j.memsci.2019.117607 (2020).
2. Abdelkareem, M. A., El Haj Assad, M., Sayed, E. T. & Soudan, B. Recent progress in the use of renewable energy sources to power water desalination plants. *Desalination* **435**, 97–113 (2018).
3. Kim, J., Park, K., Yang, D. R. & Hong, S. A comprehensive review of energy consumption of seawater reverse osmosis desalination plants. *Appl. Energy* **254**, 113652 (2019).
4. Chougradi, A. et al. Batch reverse osmosis desalination modeling under a time-dependent pressure profile. *Membranes* **11**, 1–20 (2021).
5. Peñate, B. & García-Rodríguez, L. Current trends and future prospects in the design of seawater reverse osmosis desalination technology. *Desalination* **284**, 1–8 (2012).
6. Gao, L., Yoshikawa, S., Iseri, Y., Fujimori, S. & Kanae, S. An economic assessment of the global potential for seawater desalination to 2050. *Water* **9**, 763 (2017).
7. Tu, K. L., Chivas, A. R. & Nghiem, L. D. Effects of membrane fouling and scaling on boron rejection by nanofiltration and reverse osmosis membranes. *Desalination* **279**, 269–277 (2011).
8. Fortunato, L. et al. Fouling investigation of a full-scale seawater reverse osmosis desalination (SWRO) plant on the Red Sea: membrane autopsy and pretreatment efficiency. *Desalination* **496**, 114536 (2020).
9. Susanto, H., Franzka, S. & Ulbricht, M. Dextran fouling of polyethersulfone ultrafiltration membranes—causes, extent and consequences. *J. Membr. Sci.* **296**, 147–155 (2007).
10. Bucs, S. S., Valladares Linares, R., Vrouwenvelder, J. S. & Picioreanu, C. Biofouling in forward osmosis systems: an experimental and numerical study. *Water Res.* **106**, 86–97 (2016).
11. Miyakawa, H. et al. Reliable sea water RO operation with high water recovery and no-chlorine/no-SBS dosing in Arabian gulf, Saudi Arabia. *Membranes* **11**, 1–13 (2021).
12. Shih, W. Y., Rahardianto, A., Lee, R. W. & Cohen, Y. Morphometric characterization of calcium sulfate dihydrate (gypsum) scale on reverse osmosis membranes. *J. Membr. Sci.* **252**, 253–263 (2005).
13. Tang, C. Y., Kwon, Y. N. & Leckie, J. O. Fouling of reverse osmosis and nanofiltration membranes by humic acid—effects of solution composition and hydrodynamic conditions. *J. Membr. Sci.* **290**, 86–94 (2007).
14. Ling, B., Xie, P., Ladner, D. & Battiato, I. Dynamic modeling of fouling in reverse osmosis membranes. *Membranes* **11**, 349 (2021).

15. Pontié, M. et al. Tools for membrane autopsies and antifouling strategies in seawater feeds: a review. *Desalination* **181**, 75–90 (2005).
16. Henthorne, L. & Boysen, B. State-of-the-art of reverse osmosis desalination pretreatment. *Desalination* **356**, 129–139 (2015).
17. Prihasto, N., Liu, Q. F. & Kim, S. H. Pre-treatment strategies for seawater desalination by reverse osmosis system. *Desalination* **249**, 308–316 (2009).
18. Yurt, A. & Aykın, Ö. Diphenolic Schiff bases as corrosion inhibitors for aluminium in 0.1M HCl: potentiodynamic polarisation and EQCM investigations. *Corros. Sci.* **53**, 3725–3732 (2011).
19. Popova, A., Christov, M. & Vasilev, A. Mono- and dicationic benzothiazolic quaternary ammonium bromides as mild steel corrosion inhibitors. Part II: Electrochemical impedance and polarisation resistance results. *Corros. Sci.* **53**, 1770–1777 (2011).
20. Guigui, C., Rouch, J. C., Durand-Bourlier, L., Bonnelye, V. & Aptel, P. Impact of coagulation conditions on the in-line coagulation/UF process for drinking water production. *Desalination* **147**, 95–100 (2002).
21. Sun, C., Xie, L., Li, X., Sun, L. & Dai, H. Study on different ultrafiltration-based hybrid pretreatment systems for reverse osmosis desalination. *Desalination* **371**, 18–25 (2015).
22. Baig, M. B. & Al Kutbi, A. A. Design features of a 20 migd SWRO desalination plant, A1 Jubail, Saudi Arabia. *Desalination* **118**, 5–12 (1998).
23. Zeino, A., Albakri, M., Khaled, M. & Zarzour, M. Comparative study of the synergistic effect of ATMP and DTPMPA on $CaSO_4$ scale inhibition and evaluation of induction time effect. *J. Water Process Eng.* **21**, 1–8 (2018).
24. Matin, A., Khan, Z., Zaidi, S. M. J. & Boyce, M. C. Biofouling in reverse osmosis membranes for seawater desalination: phenomena and prevention. *Desalination* **281**, 1–16 (2011).
25. Surawanvijit, S., Rahardianto, A. & Cohen, Y. An integrated approach for characterization of polyamide reverse osmosis membrane degradation due to exposure to free chlorine. *J. Membr. Sci.* **510**, 164–173 (2016).
26. Ayoub, G. M., Zayyat, R. M. & Al-Hindi, M. Precipitation softening: A pretreatment process for seawater desalination. *Environ. Sci. Pollut. Res. Int.* **21**, 2876–2887 (2014).
27. Ayoub, G. M., Hamzeh, A. & Semerjian, L. Post-treatment of tannery wastewater using lime/bittern coagulation and activated carbon adsorption. *Desalination* **273**, 359–365 (2011).
28. Boukhoubza, F. et al. Application of lime and calcium hypochlorite in the dephenolisation and discolouration of olive mill wastewater. *J. Environ. Manag.* **91**, 124–132 (2009).
29. Chen, Q., Luo, Z., Hills, C., Xue, G. & Tyrer, M. Precipitation of heavy metals from wastewater using simulated flue gas: sequent additions of fly ash, lime and carbon dioxide. *Water Res.* **43**, 2605–2614 (2009).
30. Cui, J., Du, Y., Xiao, H., Yi, Q. & Du, D. A new process of continuous three-stage co-precipitation of arsenic with ferrous iron and lime. *Hydrometallurgy* **146**, 169–174 (2014).
31. Georgiou, D., Aivazidis, A., Hatiras, J. & Gimouhopoulos, K. Treatment of cotton textile wastewater using lime and ferrous sulfate. *Water Res.* **37**, 2248–2250 (2003).
32. Lee, M., Paik, I. S., Kim, I., Kang, H. & Lee, S. Remediation of heavy metal contaminated groundwater originated from abandoned mine using lime and calcium carbonate. *J. Hazard. Mater.* **144**, 208–214 (2007).
33. Ayoub, G. M. & Merhebi, F. Characteristics and quantities of sludge produced by coagulating wastewater with seawater bittern, lime and caustic. *Adv. Environ. Res.* **6**, 277–284 (2002).
34. Desjardins, C., Koudjonou, B. & Desjardins, R. Laboratory study of ballasted flocculation. *Water Res.* **36**, 744–754 (2002).
35. Brahmi, K. et al. Treatment of heavy metal polluted industrial wastewater by a new water treatment process: ballasted electroflocculation. *J. Hazard. Mater.* **344**, 968–980 (2018).
36. Chhuon, R., Shahid, M. K., Kim, S. & Choi, Y. Mill scale as a ballasted flocculant for enhancing the settleability of activated sludge. *J. Environ. Chem. Eng.* **8**, https://doi.org/10.1016/j.jece.2020.104237 (2020).
37. Sieliechi, J., Lartiges, B., Skali-Lami, S., Kayem, J. & Kamga, R. Floc compaction during ballasted aggregation. *Water Res.* **105**, 361–369 (2016).
38. Plum, V. et al. The actiflo method. *Water Sci. Technol.* **37**, 269–275 (1998).
39. Lapointe, M. & Barbeau, B. Characterization of ballasted flocs in water treatment using microscopy. *Water Res.* **90**, 119–127 (2016).
40. Denieul, M.-P. et al. Industrial waste waters re-use: application of 3FM® high speed filtration and high rate softening as pre-treatment of wastewaters from the high water consuming pulp&Paper sector. *Proc. Water Environ. Fed.* **2011**, 5136–5150 (2012).
41. Vaxelaire, J. & Olivier, J. Conditioning for municipal sludge dewatering. From filtration compression cell tests to belt press. *Dry. Technol.* **24**, 1225–1233 (2006).
42. Chua, K. T., Hawlader, M. N. A. & Malek, A. Pretreatment of seawater: results of pilot trials in Singapore. *Desalination* **159**, 225–243 (2003).
43. Chen, K. L., Song, L., Ong, S. L. & Ng, W. J. The development of membrane fouling in full-scale RO. *Process. J. Membr. Sci.* **232**, 63–72 (2004).
44. Mucha, J. Characteristics of grey water filtration on polypropylene filters. *Ecol. Chem. Eng.* **22**, 39–50 (2015).
45. Comstock, S. E. H., Boyer, T. H. & Graf, K. C. Treatment of nanofiltration and reverse osmosis concentrates: comparison of precipitative softening, coagulation, and anion exchange. *Water Res.* **45**, 4855–4865 (2011).
46. Lu, J., You, S. & Wang, X. Forward osmosis coupled with lime-soda ash softening for volume minimization of reverse osmosis concentrate and $CaCO_3$ recovery: A case study on the coal chemical industry. *Front. Environ. Sci. Eng.* **15**, 1–10 (2021).
47. Zhang, L. et al. Impact of influent deviations on polymer coagulant dose in warm lime softening of synthetic SAGD produced water. *Water Res.* **200**, 117202 (2021).
48. Xiang, G., Ye, W., Yu, F., Wang, Y. & Fang, Y. Surface fractal dimension of bentonite affected by long-term corrosion in alkaline solution. *Appl. Clay Sci.* **175**, 94–101 (2019).
49. Marsilio, V., Russi, F., Iannucci, E. & Sabatini, N. Effects of alkali neutralization with CO_2 on fermentation, chemical parameters and sensory characteristics in Spanish-style green olives (Olea europaea L.). *LWT Food Sci. Technol.* **41**, 796–802 (2008).
50. Quevedo, N. et al. Reverse osmosis pretreatment alternatives: demonstration plant in the seawater desalination plant in Carboneras, Spain. *Desalination* **265**, 229–236 (2011).

ACKNOWLEDGEMENTS

Nishihara Environment Co., Ltd. provided the experimental materials. We thank everybody who participated in this project. This study received no specific grant from funding agencies in the public, commercial, or not-for-profit sectors.

AUTHOR CONTRIBUTIONS

T.Y.: Investigation, Data Analysis, and Writing - Original Draft. Y.S.: Conceptualization, Methodology, Investigation, Writing - Original Draft, Review & Editing, and Supervision.

COMPETING INTERESTS

The authors declare no competing interests.

ADDITIONAL INFORMATION

Supplementary information The online version contains supplementary material available at https://doi.org/10.1038/s41545-023-00226-0.

Correspondence and requests for materials should be addressed to Yoshihiro Suzuki.

Reprints and permission information is available at http://www.nature.com/reprints

Publisher's note Springer Nature remains neutral with regard to jurisdictional claims in published maps and institutional affiliations.